Available online at www.sciencedirect.com
ScienceDirect
International Journal of Pharmaceutics 347 (2008) 62–70
INTERNATIONAL JOURNAL OF PHARMACEUTICS
www.elsevier.com/locate/ijpharm

Theoretical and experimental investigations of organic acids/cyclodextrin complexes and their consequences upon the formation of miconazole/cyclodextrin/acid ternary inclusion complexes

Valéry Barillaro [a,*,1], Georges Dive [b,1], Pascal Bertholet [a], Brigitte Evrard [a], Luc Delattre [a], Michel Frederich [c], Eric Ziémons [d], Geraldine Piel [a]

[a] *Laboratory of Pharmaceutical Technology, Department of Pharmacy, University of Liege, CHU-Tour 4, Bât. B36, Avenue de l'Hôpital 1, B-4000 Liège, Belgium*
[b] *Center for Protein Engineering, Chemical Department, University of Liege, Bât B6, Allée de la Chimie 3, B-4000 Liège, Belgium*
[c] *Laboratory of Pharmacognosy, Natural and Synthetic Drug Research Center, University of Liege, CHU-Tour 4, Bât. B36, Avenue de l'Hôpital 1, B-4000 Liège 1, Belgium*
[d] *Laboratory of Analytical Chemistry, Department of Pharmacy, University of Liege, CHU-Tour 4, Bât. B36, Avenue de l'Hôpital 1, B-4000 Liège, Belgium*

Received 24 May 2007; received in revised form 18 June 2007; accepted 19 June 2007
Available online 24 June 2007

Abstract

^{1}H NMR spectrometry, FT-IR spectroscopy, as well as molecular modeling at the AM1 level and normal mode analysis were used to characterise the interactions and the formation of inclusion complexes between three organic acids: maleic, fumaric, L-tartaric acids and βCD. In aqueous medium, the complexation was confirmed by ^{1}H NMR spectroscopy using two-dimensional technique. The stable geometries of the complexes were determined by molecular modeling. Experimental infrared frequencies were assigned on the base of the vibrational normal mode calculation at the fully optimized geometry for the inclusion complexes. All the results point out the presence of stable inclusion complexes between acids and βCD at the solid state. These results show the double role of the acid. Correlated with the theoretical and experimental data previously obtained for the miconazole/CD/acids complexes, in function of both acids and CDs structures, the acids can either stabilize the complexes by formation of a multicomponent complex or form acid/CD inclusion complexes, hindering the guest inclusion.

Keywords: Acids; Cyclodextrins; ROESY experiments; Molecular modeling; Normal mode; FT-IR; Supercritical carbon dioxide; AM1 calculations

1. Introduction

It is well described in the literature that cyclodextrins (CDs) can be used as solubilizing agents for drugs which present a poor aqueous solubility (Loftsson and Brewster, 1996). This solubility can be enhanced by the use of a low molecular weight organic acid which stabilizes the drug/CD complex but also which increases the solubility of the basic drug by salt formation (Redenti et al., 2000). The solubilization of miconazole by means of CDs is well described (Bononi, 1990; Mura et al., 1992). When an acidic ternary compound is used, a synergistic effect between acids and CDs occurs. Indeed, the miconazole solubility in presence of both acid and CD is greater than the expected one by adding the effects of CD and acid separately (Piel et al., 1998). In a previous study, the inclusion of miconazole into several cyclodextrins using supercritical carbon dioxide processing has been studied and the influence of both CDs and organic acids on the inclusion yield has been determined. The results show that the inclusion yields were dramatically improved when an acid and a hydroxypropylated CD were used. By opposite, when a natural CD was used such as βCD and γCD, this effect was much weaker (Barillaro et al., 2004).

In a recent paper, molecular modeling was used to elucidate the role of several types of acid during the formation of miconazole ternary inclusion compounds. The results have shown that,

* Corresponding author. Tel.: +32 4 366 43 01; fax: +32 4 366 43 02.
E-mail address: v.barillaro@gmail.com (V. Barillaro).
[1] These authors contributed equally to this study.

0378-5173/$ – see front matter © 2007 Elsevier B.V. All rights reserved.
doi:10.1016/j.ijpharm.2007.06.030

depending on its structure, the acid can either stabilize the inclusion complex or extract miconazole from the CD cavity, especially when L-tartaric acid and natural CD were used, as βCD, confirming the experimental observations (Barillaro et al., 2007).

The interactions between organic acid and cyclodextrins have been already studied in the literature but these studies are limited to the determination of stability constant of the acid/CD complex using solubility diagram (Fenyvesi et al., 1999), freezing point depression (Suzuki et al., 1993), pH-potentiometric titration (Csernàk et al., 2005) and calorimetry (Germain et al., 1995). These reports suggest the formation of inclusion complexes. In fact, all the results show the existence of an interaction between acids and CD but the nature of this interaction is uncertain. Up to now, to our knowledge, there is no explicit proof of the formation of a genuine inclusion complex.

This work is then focused on the elucidation of the interactions between maleic, fumaric or L-tartaric acids and βCD. Experimental and theoretical data will support this study. Acid/CD systems were investigated by ^{1}H NMR spectroscopy, infrared spectroscopy, molecular modeling using the AM1 semiempirical method. Eventually, the consequences of these results on the formation of miconazole/CD/acid inclusion complexes were evaluated.

2. Materials and methods

2.1. Materials

βCD (Eur. Ph. fourth ed., 7.58% H2O) was kindly supplied by Roquette (Lestrem, France). Fumaric acid was from Fluka (Buchs, Switzerland), maleic acid from Acros (New Jersey, USA) and L-tartaric acid (Eur Ph. fourth ed.) from Merck (Damstadt, Germany). Deuterium oxide (99.97%) was purchased from Eur-isotop (Saint-Aubain, France). CO_2 was of N48 quality (99.998%) from Air Liquide (Liege, Belgium). All the products were used as received.

2.2. Methods

2.2.1. ^{1}H NMR studies

One-dimensional ^{1}H NMR spectra were recorded at 25 °C on a Bruker Avance 500 operating at a proton NMR frequency of 500.13 MHz using a 5 mm probe and a simple pulse-acquire sequence. Acquisition parameters consisted of a sweep width of 10,333.6 Hz, a pulse width of 7.7 μs, an acquisition time of 3.14 s and a relaxation delay of 1 s. One hundred twenty-eight scans were recorded. FIDs were Fourier transformed with LB = 0.3 Hz and GB = 0. The resonance at 4.800 ppm due to residual solvent (HOD) was used as internal reference.

Reference solutions were prepared by separately dissolving an appropriate amount of maleic, fumaric, L-tartaric acids and βCD, directly in 600 μL D_2O in order to obtain a concentration of 10 mM. The resulting solutions were then transferred in the 5 mm RMN tubes.

Sample solutions were prepared by dissolving maleic acid and βCD in 600 μL D_2O in order to obtain the final concentration of 10 mM (maleic acid:CD molar ratio 1:1). The same procedure was applied for the fumaric acid. But, for L-tartaric acid due to the weak interaction with βCD, the L-tartaric acid concentration was increased up to 20 mM and the resulting molar ratio was 2:1 (L-tartaric acid 20 mM and βCD 10 mM).

^{1}H NMR chemical shifts ($\Delta\delta$) caused upon complexation were measured to confirm the inclusion of acids and calculated according to the following formula: $\Delta\delta = \delta_{(free)} - \delta_{(complex)}$.

2.2.2. ROESY experiments

ROESY (Rotating-frame Overhauser Effect SpectroscopY) spectra were acquired in the phase sensitive mode using the same spectrometer. Each spectrum consisted of a matrix of 2K (F2) by 1K (F1) covering a spectral width of 5122 Hz. Spectra were obtained from the samples solutions prepared for the ^{1}H NMR studies, using a spin-lock mixing periods of 350 ms for the maleic acid/βCD and fumaric acid/βCD systems, and of 400 ms for the L-tartaric acid/βCD system. For the last system, as the resonance of the L-tartaric acid protons is close to that of the residual solvent, a sequence of presaturation was used. Before Fourier transformation, the sine apodization function was applied in both dimensions. Sixty-four scans were collected for each of the 256 experiments.

2.2.3. Molecular modelling

2.2.3.1. Docking studies. The geometry optimisation was performed with the Gaussian 98 package (Frisch et al., 1998) by using semiempirical AM1 (Austin Model 1) method (Dewar et al., 1985). The geometries were fully optimized without any constraint by minimisation of the analytical gradient. The nature of the located critical points is determined by vibrational frequency calculation derived from the second derivative matrix. When all the eigenvalues of this Hessian matrix are positive, the energy is minimum in each direction associated to the variables. For each equilibrium structure, the thermochemistry data are derived from the analytical frequency calculation at 298.15 K and 1 atm. (Mc Quarrie, 1973).

The same procedure was used in the study of miconazole, cyproterone acetate and RO 28–2653 inclusion complexes (Piel et al., 2001; Henry de Hassonville et al., 2004; Bertholet et al., 2005; Barillaro et al., 2007). Starting from the optimized geometry local minimum of each complex, acid and CD were re-optimized separately. This procedure allows the determination of consistent energetic data, as each relative energy is calculated by reference to the geometry of the complex.

2.2.3.2. Normal modes analysis. For infrared spectrum of the complexes, vibrational frequencies and intensities were determined by finite differences. All the calculated frequencies are positive assuring that the calculated geometry is indeed a local minimum. Calculated harmonic vibrational frequencies were scaled down by a factor of 0.9532 (Scott and Radom, 1996). To visualize the normal modes, the Molden v. 3.5 software for Windows® was used (Schaftenaar and Noordik, 2000). To compare with the experimental results, simulated IR spectra were calculated using the Swizard program revision 4.1 (Gorelsky, 2005) using the Lorentzian model. The

half-bandwidths ($\Delta_{1/2,I}$) were arbitrarily taken to be equal to $10\,cm^{-1}$.

2.2.4. FT-IR

The transmission IR spectra were recorded from isotopically dispersed products in KBr. The FTIR spectra were collected over the spectral region 4000–600 cm^{-1} at a resolution of 4 cm^{-1} and intervals of 0.5 cm^{-1} on a computer interfaced Bruker Tensor 27 FTIR spectrophotometer equipped with a liquid N_2-cooled MCT detector. The number of scan is 64.

2.2.5. Preparation of acid/CD physical mixtures and complexes

The physical mixtures between acid and βCD were prepared by gently grinding, in a mortar, the caculated and exactly weighed amounts of compounds in equimolar ratio.

The solid inclusion complexes were produced using supercritical carbon dioxide following a method and an experimental set-up previously described (Barillaro et al., 2004). The physical mixtures, prepared as described above, were processed by supercritical carbon dioxide in a static mode at 30 MPa, 125 °C during 60 min.

3. Results and discussion

3.1. NMR studies

For each acid, the difference in the chemical shift between the free βCD, acid and the complex has been determined.

Two-dimensional ROESY experiments have often been successfully applied to prove through-space intermolecular interactions in CD complexes. Indeed, in the ROESY experiments, dipolar interactions between protons at a distance less than 3–4 Å are detected as cross-peaks in a bi-dimensional map, indicating the portion of the guest situated in the torus cavity (Schneider et al., 1998). In this study, ROESY spectra were collected to gain additional insights. The effects were only qualitatively used.

3.1.1. Maleic acid

In the spectrum of maleic acid, the ethylenic protons give rise to one resonance located at 6.249 ppm (singlet).

Table 1 reports the chemical shift values of maleic acid and βCD protons in the native and complexed forms. Recordable downfield shifts are observed in the maleic acid spectrum. Moreover, in the presence of maleic acid, both H3 and H5 protons of the βCD are shifted upfield. Because these protons are inside the βCD cavity, their shifts suggest that the acid is included inside the βCD (Djedaïni and Perly, 1990). The signals due to H1, H2, H4 and H6 are also upfield shifted but these shifts are less pronounced. So, the upfiled shifts of the protons located inside the cavity of the βCD (H3 and H5) and the minor modifications of those located at the outside of the torus evidence the existence of an interaction between the CD cavity and the guest, hence complexation.

The ROESY spectrum of the maleic acid/βCD is depicted in Fig. 1. The cross-peak between the H3 and H5 protons of the βCD and the proton of maleic acid demonstrates the inclusion of maleic acid into the βCD cavity.

Table 1
^{1}H chemical shifts corresponding to maleic acid and βCD in free and in complexed state

Protons	$\delta_{(free)}$	$\delta_{(complex)}$	$\Delta\delta$[a]
βCD			
H1	5.142	5.133	0.009
H2	3.722	3.713	0.009
H3	4.035	4.024	0.011
H4	3.654	3.646	0.008
H5	3.926	3.913	0.013
H6	3.950	3.942	0.008
Maleic acid			
H	6.249	6.460	−0.211

[a] $\Delta\delta = \delta_{(free)} - \delta_{(complex)}$.

3.1.2. Fumaric acid

As for maleic acid, fumaric acid protons give rise to one singlet at 6.684 ppm.

Recordable downfield shifts are observed in the fumaric acid and recordable upfield shifts in the βCD one (Table 2). The highest difference (0.016 ppm) is observed on the H3 protons of the βCD. Only the H3 proton, located inside the CD cavity, is appreciably shifted upfield. For the other CD protons, the upfield shifts are less pronounced. So, these observations evidence the existence of an interaction between the guest, fumaric acid, and the inside of the βCD, demonstrating the complexation.

Fig. 2 depicted the ROESY spectrum of the fumaric acid/βCD complex. A cross-peak between the proton of fumaric acid and H3 and H5 of the βCD is observed. This confirmed the intermolecular interaction between the acid and the βCD cavity.

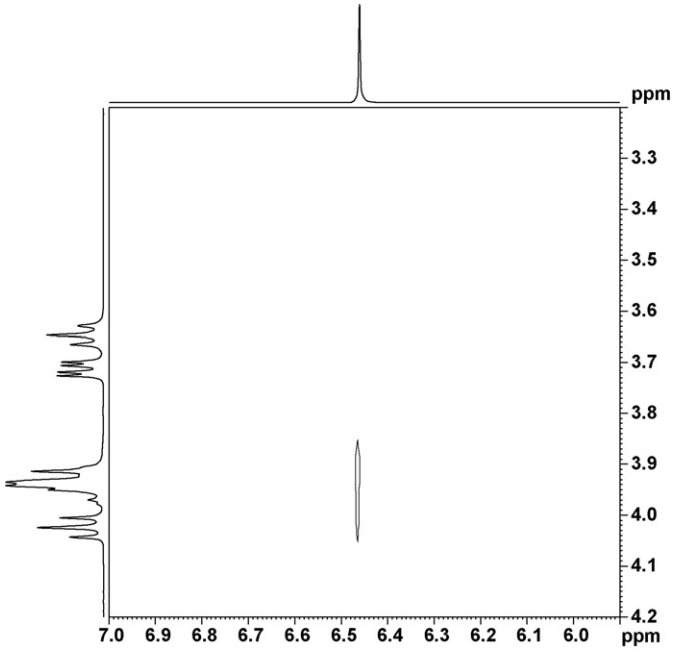

Fig. 1. Expansion from the ROESY spectrum of the maleic acid/βCD complex.

Table 2
^{1}H chemical shifts corresponding to fumaric acid and βCD in free and in complexed state

Protons	$\delta_{(free)}$	$\delta_{(complex)}$	$\Delta\delta^a$
βCD			
H1	5.142	5.135	0.007
H2	3.722	3.716	0.006
H3	4.035	4.019	0.016
H4	3.654	3.651	0.003
H5	3.926	3.918	0.008
H6	3.950	3.941	0.009
Fumaric acid			
H	6.684	6.784	−0.100

[a] $\Delta\delta = \delta_{(free)} - \delta_{(complex)}$.

Table 3
^{1}H chemical shifts corresponding to L-tartaric acid and βCD in free and in complexed state

Protons	$\delta_{(free)}$	$\delta_{(complex)}$	$\Delta\delta^a$
βCD			
H1	5.142	5.102	0.040
H2	3.722	3.672	0.050
H3	4.035	3.995	0.040
H4	3.654	3.615	0.039
H5	3.926	3.891	0.035
H6	3.950	3.910	0.040
L-Tartaric acid			
H	4.555	4.722	−0.167

[a] $\Delta\delta = \delta_{(free)} - \delta_{(complex)}$.

3.1.3. L-tartaric acid

The aliphatic protons of L-tartaric acid appear at 4.555 ppm (singlet).

The chemical shifts for both free and complexed state for L-tartaric acid and βCD are listed in Table 3. As previously observed, downfield shift is observed in the L-tartaric acid spectrum and upfield shifts in the βCD spectrum. The differences are very high and between 0.039 and 0.050 ppm while the highest is observed for H2 proton. In this case, the βCD protons seem to shift in the same magnitude. This can be explained by the high concentration of L-tartaric acid which is 20 mM in contrast to the one of βCD which is 10 mM. So, the interactions with the outside and the inside of the CD cavity can occur with the same probability. This fact can be correlated with the little stability constant of the L-tartaric acid/βCD complex. Indeed, Suzuki et al. reported a stability constant of 7.8 M^{-1} for this complex while it is 18.2 M^{-1} for maleic acid/βCD complex and 53.6 M^{-1} for fumaric acid/βCD complex (Suzuki et al., 1993; Csernàk et al., 2005).

Fig. 3 depicted the ROESY spectrum of fumaric acid/βCD complex. Surprisingly, a cross-peak between H3 and H5 proton of the CD and the L-tartaric acid proton appears. These two intermolecular cross-peaks evidence the complexation of L-tartaric acid into the CD cavity.

3.2. Molecular modeling

The results are presented as energetic outcome expressed as complexation, deformation and interaction energies. The complexation energy is the difference between the energy of the complex and the sum of both partners (acid and CD) in their respective equilibrium geometry. The deformation energy is determined by the difference between the energy of the partners of the complex at their respective equilibrium geometry and their energy at the complex geometry. The interaction energy is defined as the difference between the energy of the complex and the sum of the energies of both partners at their complex geometry. The optimized geometries of the three complexes are

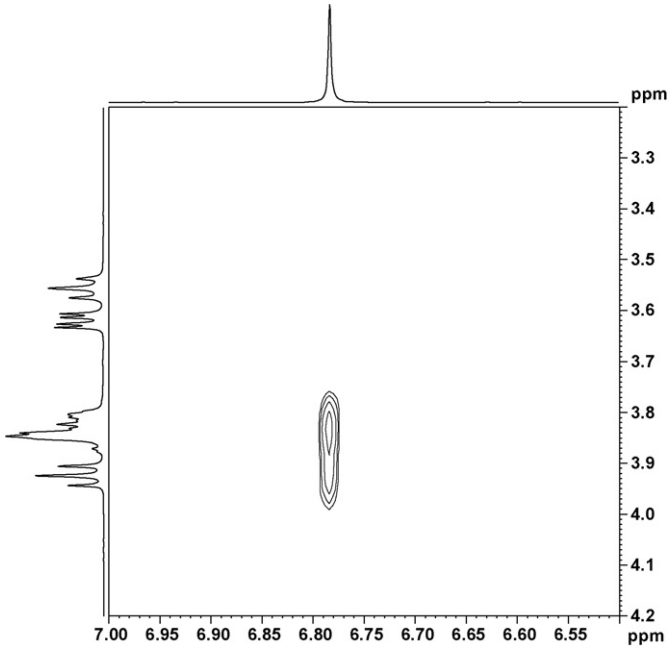

Fig. 2. Expansion from the ROESY spectrum of the fumaric acid/βCD complex.

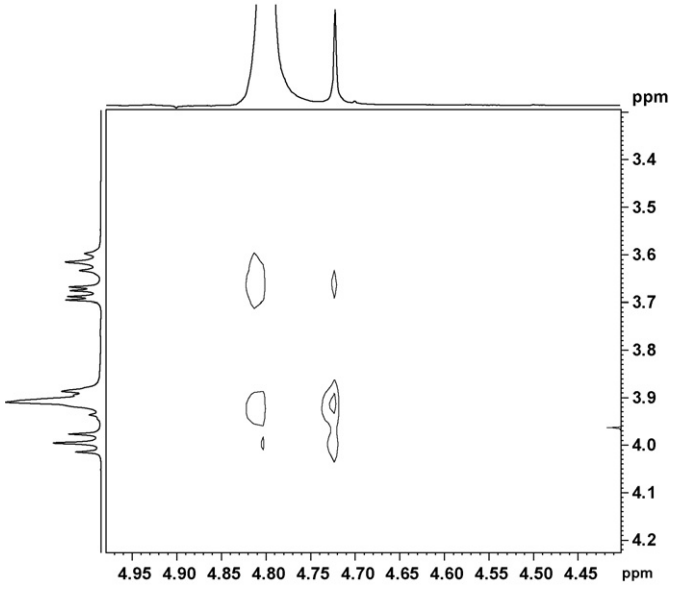

Fig. 3. Expansion from the ROESY spectrum of the L-tartaric acid/βCD complex.

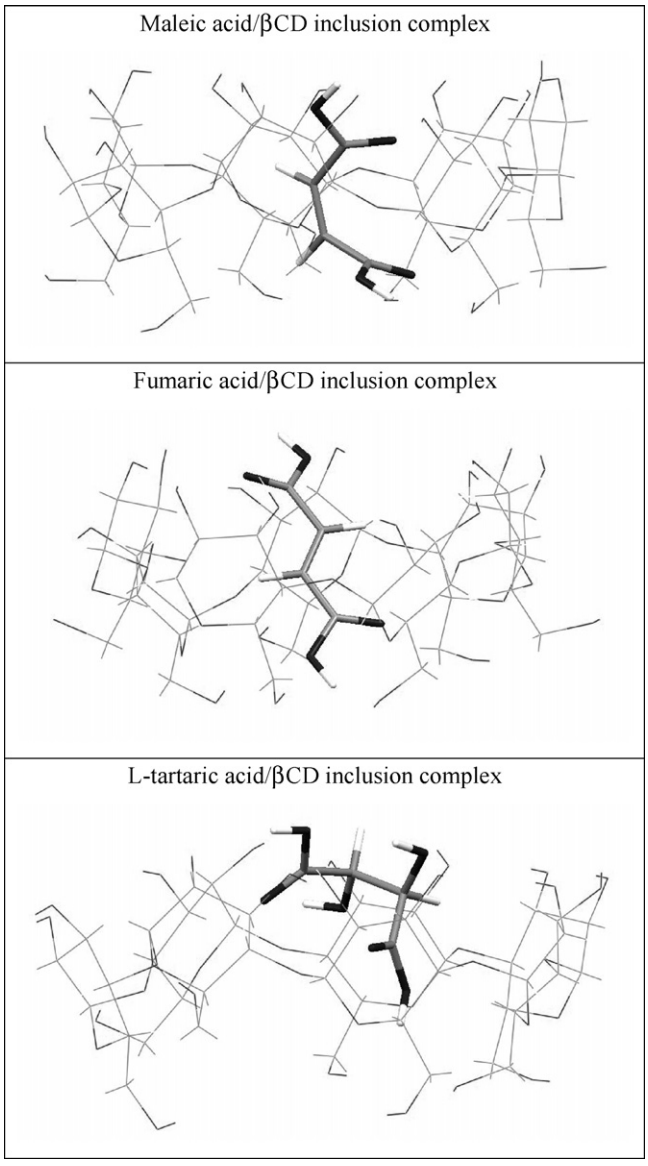

Fig. 4. Optimized structures of the acids/βCD complexes. Maleic acid/βCD inclusion complex. Fumaric acid/βCD inclusion complex. L-Tartaric acid/βCD inclusion complex.

depicted in Fig. 4. Energies, entropy and enthalpy are presented in Table 4.

As observed for all the studied complexes, the difference of free energy (ΔG) is positive indicating that a contribution of energy is necessary to form these complexes. Some interesting interatomic distances could be pointed out on optimized complexes. The formation of hydrogen bond between the acid and the CD can be observed. Indeed, a distance less than 3 Å between a nitrogen or an oxygen and hydrogen (aliphatic or not) allows the formation of a bond which stabilizes the complex (Dive et al., 1993).

The results show that maleic acid forms a stable complex with βCD ($\Delta E < 0$). The interaction energy is high and equal to −14.339 kcal/mol. This feature is correlated with the formation of numerous hydrogen bonds between maleic acid and βCD which consolidates the inclusion complex and improves the

Table 4
Complexation, deformation and interaction energies in kcal/mol (ΔS in cal/mol K) with the reference to both reoptimized βCD and acid[a]

Model	Maleic acid/βCD	Fumaric acid/βCD	L-Tartaric acid/βCD
Complexation energy			
ΔE	−11.199	−6.479	−5.415
ΔH	−9.115	−4.654	−1.007
ΔS	−51.186	−49.411	−65.198
ΔG	6.147	10.078	18.432
Deformation energy			
Acid	−1.122	−0.986	−4.192
βCD	−2.078	−5.022	−9.250
Interaction energy	−14.399	−12.488	−18.857

[a] Interaction energy: energy of the complex — sum of the energy of each partner at the complex geometry. Deformation energy: energy of the partner — energy of the partner in the complex. Complexation energy: energy of the complex — sum energy of each part in their respective equilibrium geometry. ΔG is calculated at 298.15 K.

Table 5
Interatomic distances (Å) between some functions of maleic acid and βCD able to form hydrogen bonds

Maleic acid	βCD	Distance (Å)
C—O	O—H 2	2.351
O—H	O—H 3	2.205
C=O	C—H 3	2.546
C—H	C—O 6	2.308
O—H	C—O 6	2.143
C=O	O—H 6	2.201

interaction and also the complexation energy value (Table 5). As we can see, C=O, O–H and ethylenic C–H functions of maleic acid are involved in the formation of hydrogen bonds with the βCD. Moreover, the deformation energy is weak. The feature can promote the inclusion.

For fumaric acid/βCD complex, Table 4 shows that the complexation energy is stabilizing ($\Delta E < 0$). Moreover, the interaction energy is high (−12.488 kcal/mol) and, as observed for the maleic acid/βCD complex, this high value is due to hydrogen bonds formation between fumaric acid and βCD (Table 6). As seen for the previous complex, C=O, C–O and O–H functions of the fumaric acid form hydrogen bonds with the βCD and, moreover, some of them participate in more than one hydrogen bond. The deformation energy of fumaric acid is weak, but the

Table 6
Interatomic distances (Å) between some functions of fumaric acid and βCD able to form hydrogen bonds

Fumaric acid	βCD	Distance (Å)
C=O	O—H 2	2.229
C—O	O—H 2	2.277
C—O	C—H 3	2.336
O—H	C—O 3	2.395
C=O	C—H 5	2.452
C—O	O—H 6	2.267
C—O	O—H 6	2.293
O—H	C—O 6	2.144

Table 7
Interatomic distances (Å) between some functions of L-tartaric acid and βCD able to form hydrogen bonds

L-Tartaric acid	βCD	Distance (Å)
C═O	C—H 3	2.237
C═O	O—H 2	2.132
O—H carb	C—O 2	2.129
C—O carb	O—H 2	2.537
C—O alc	C—H 3	2.271
O—H alc	O—H 2	2.152
C—O alc	C—H 3	2.825
C═O	O—H 3	2.229
C—O carb	C—H 5	2.377
O—H alc	C—O 6	2.174

one of the βCD is much higher (−5.022 kcal/mol). βCD needs more energy to fit its shape in the complex than fumaric acid.

L-tartaric acid/βCD complex also exhibits a stabilizing complexation energy ($\Delta E < 0$; Table 4). Surprisingly, the energies of deformation are very high, −4.192 kcal/mol for L-tartaric acid and −9.250 kcal/mol for βCD. So, the guest and the host need much energy to adapt their shapes at the complexed state. The high level of interaction energy is explained by the formation of much more hydrogen bonds between the L-tartaric acid and the βCD than in the other studied complexes. These interactions are listed in Table 7.

In conclusion, all the studied complexes show stabilizing complexation energies and the highest value is observed for the maleic acid/βCD complex. This last complex also shows the weaker deformation energy and higher interaction energy. So, the stability of the complexes is in the order: maleic acid/βCD > fumaric acid/βCD > L-tartaric acid/βCD.

3.3. Theoretical and experimental vibrational study of the acids/βCD complexes

In order to understand the behaviour of acids during the supercritical carbon dioxide treatment, acids/βCD physical mixtures were processed with the same procedure that has been applied to miconazole/CD(/acid) complexes (Barillaro et al., 2004). FT-IR spectra of physical mixtures and corresponding complexes were recorded.

The theoretical spectra were constructed and compared to the experimental ones.

3.3.1. Maleic acid/βCD complex

The spectra for maleic acid/βCD systems are depicted in Fig. 5. Spectral modifications are observed between the physical mixture and the complex. Indeed, the carbonyl stretching located at 1734.1 and 1706.9 cm^{-1} in the physical mixture are respectively shifted at 1732.3 and 1700.7 cm^{-1} in the complex assuming the interaction between the acid and the CD. The band at 1637.6 cm^{-1}, visible in both physical mixture and complex, is due to water contained in the sample. The theoretical spectrum of the complex confirms this hypothesis. Indeed, AM1 calculation predicts two frequencies of the C=O stretching at 1986.7 and 1967.6 cm^{-1}. The C=C stretching is predicted at 1810.8 cm^{-1}

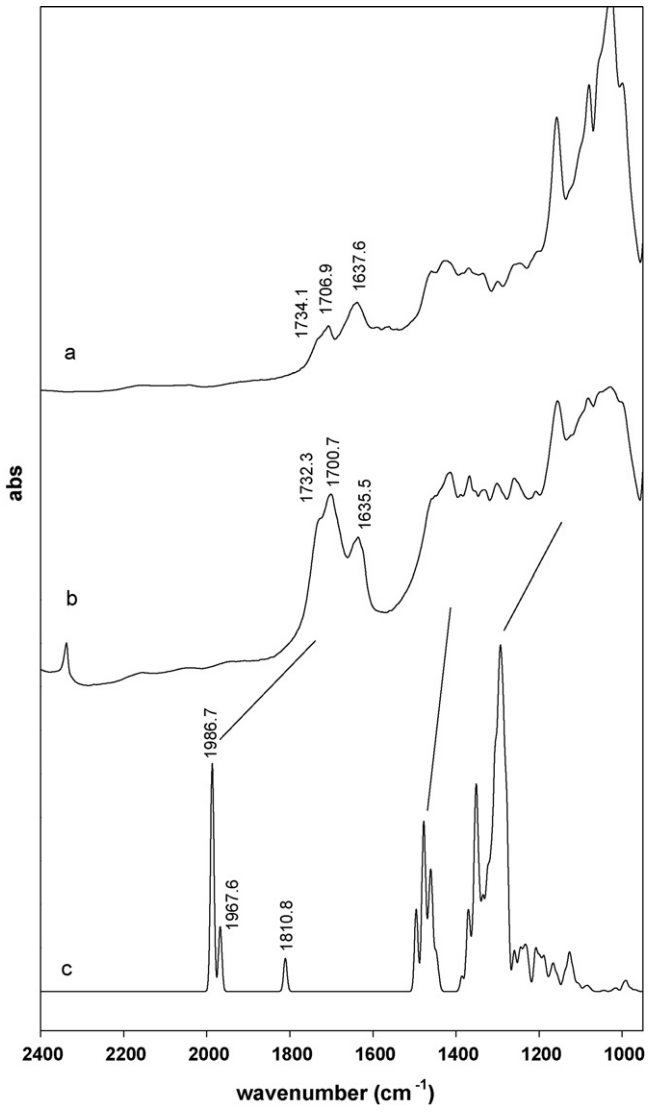

Fig. 5. Expansion of the infrared spectra for the maleic acid/βCD systems: (a) experimental spectrum of maleic acid/βCD physical mixture, (b) experimental spectrum of maleic acid/βCD complex, (c) calculated spectrum of maleic acid/βCD complex.

but is not observed in the complex spectrum. Then, deformations of the hydroxyl groups of the βCD and of the acid occur between 1495.8 and 1442.3 cm^{-1}. Finally, the deformations of the C–H of the CD and the OH deformation of the βCD and of maleic acid are calculated between 1386.6 and 1334.7 cm^{-1}. It is well known that semi-empirical and Hartree–Fock methods typically overestimate the harmonic vibrational frequencies by neglect of the correlation energy (Scott and Radom, 1996; Holder and Barley, 1993). After the application of a scaling factor of 0.9532, a residual overestimation, due to the method itself, is observed. Indeed, AM1 method allows the study of large system with an attracting computational cost, but its accuracy for predicting vibrational frequencies is about 126 cm^{-1} (Scott and Radom, 1996). So, the theoretical spectrum of the maleic acid/βCD complex is shifted after scaling but allows the assignments of the bands experimentally observed. Moreover, it is interesting to note that the optimized geometry of the complex,

starting point for the vibrational frequency calculation, represents the thermodynamically most stable geometry but, in the solid state, several other geometries can occur. This is why the bands of the experimental spectra are wider than those of the theoretical ones.

3.3.2. *Fumaric acid/βCD complex*

Fig. 6 depicts the experimental and theoretical spectra obtained for the fumaric acid/βCD systems. Again, significant spectral modifications are observable between the physical mixture and the complex. Indeed, one band observed in the physical mixture at 1670.1 cm^{-1} and assigned to C=O stretching and to water contained in the sample splits into two bands at 1706.1 and 1645.7 cm^{-1} in the complex. The shift of the band due to the C=O stretching can evidence a modification of the fumaric acid environment and thus leads to an inclusion compound. The AM1 calculation of the vibrational frequency for the complex confirms our hypothesis. The C=O stretching is predicted at 1972.8 cm^{-1}, the C=C stretching at 1790.4 cm^{-1} and is not experimentally observable. The OH deformation occurs at 1507.4 and at 1473.4 and 1455.9 cm^{-1} for the βCD. The bands between 1304.9 and 1211.2 cm^{-1} are assigned to βCD CH deformation. So, AM1 calculation provides theoretical spectrum in good agreement with the experimental one but with a shift which is intrinsic to the approximation method.

3.3.3. L-*tartaric acid/βCD complex*

The spectra recorded for the L-tartaric acid/βCD systems and the theoretical spectrum are shown in Fig. 7. In the experimental spectra, the band at 1733.7 cm^{-1} observed in the physical mixture and attributed to C=O stretching shifts to 1734.8 cm^{-1} in the complex and its intensity significantly increases. The band located at 1643.1 cm^{-1} in the physical mixture does not present any modification and is attributed to the water contained in the samples. One more time, AM1 calculation helps us to

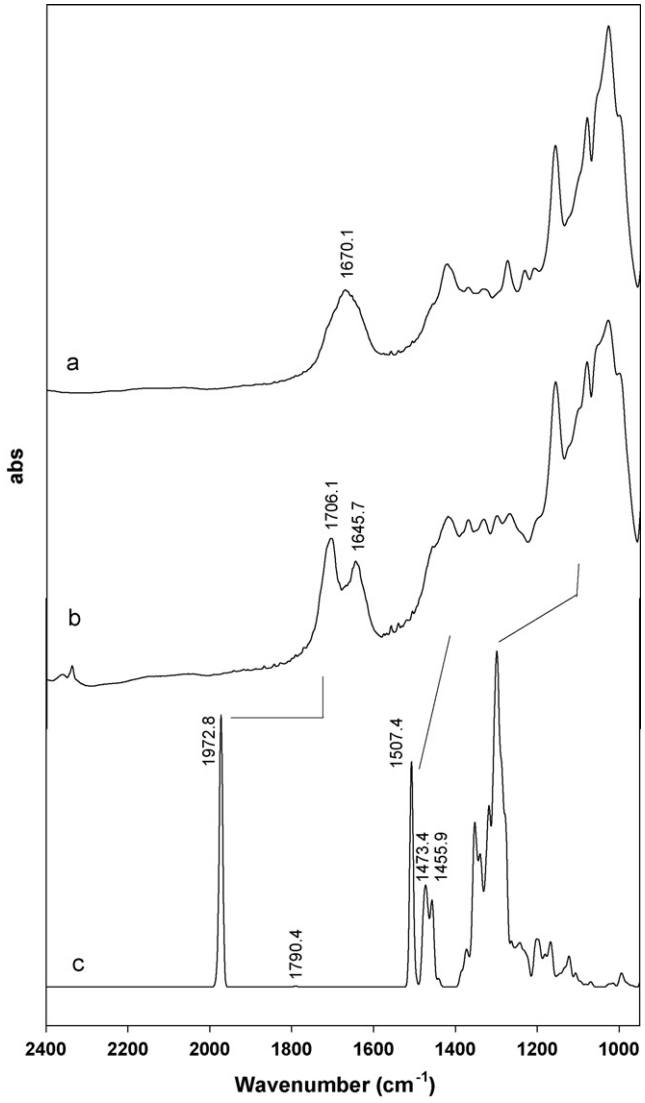

Fig. 6. Expansion of the infrared spectra for the fumaric acid/βCD systems: (a) experimental spectrum of fumaric acid/βCD physical mixture, (b) experimental spectrum of fumaric acid/βCD complex, (c) calculated spectrum of fumaric acid/βCD complex.

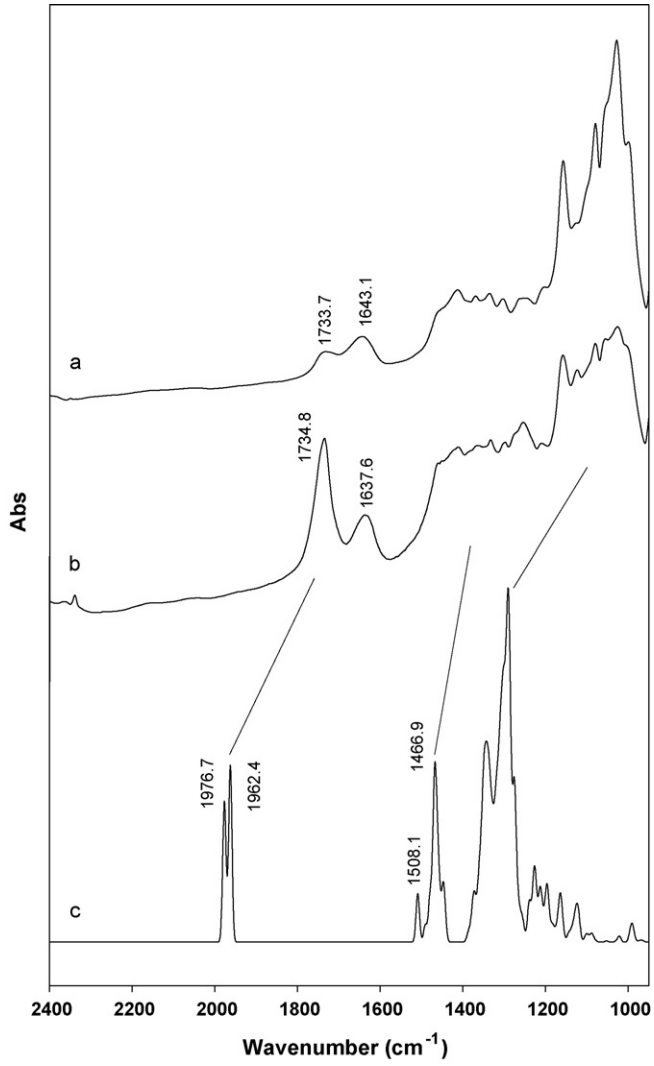

Fig. 7. Expansion of the infrared spectra for the L-tartaric acid/βCD systems: (a) experimental spectrum of L-tartaric acid/βCD physical mixture, (b) experimental spectrum of L-tartaric acid/βCD complex, (c) calculated spectrum of L-tartaric acid/βCD complex.

assign the experimental spectrum. So, AM1 method predicts two bands for C=O stretching at 1976.7 and 1962.4 cm^{-1}. The band at 1508.1 cm^{-1} is assigned to deformation of alcoholic and of the carboxylic OH group of L-tartaric acid. The bands at 1466.9 cm^{-1} is assigned to OH deformation of the βCD. Finally, the bands between 1387.8 and 1307.5 cm^{-1} are assigned to the CH deformation of the CD. So, the theoretical spectrum provided by the AM1 approximation is in good agreement with the experimental one.

3.4. Hypothesis on the influences of ternary agents on the miconazole inclusion into cyclodextrins

As reported earlier (Barillaro et al., 2004), during the formation of miconazole/CD complex using supercritical carbon dioxide, low molecular weight acids generally improve the inclusion yield. This improvement depends on several factors. The structure and also the conformation of the acidic ternary compound are very important and manage the interactions between the host and the guest. As described in a previous paper (Barillaro et al., 2007), using molecular modeling, the interactions between miconazole, CDs and acids have been studied and depend on the nature of both the acid and the CD. With βCD, maleic and fumaric acids stabilize the formation of complexes by ternary inclusion structure. But the importance of this stabilization is function of the C=C conformation. With the same CD, the situation is totally different with L-tartaric acid. Indeed, this acid extracts miconazole from the βCD cavity. By the opposite, with hydroxypropylβCD (HPβCD) and HPγCD, L-tartaric acid stabilizes the miconazole complexes. All these observations were confirmed by experimental results.

It is now possible to understand the genuine role of the acidic ternary agent in the formation of miconazole/CD complex. Indeed, during the complexation, two phenomena occur. On one hand, there is the inclusion of miconazole into CD and finally the formation of a ternary inclusion complex. On the other hand, there is also the inclusion of the acid into the CD cavity. In this case, the acid plays a competitive role, hindering the CD cavity. The balance between the two phenomena depends on the nature of both the CD and the acid. In association with βCD, there is a preferential inclusion of L-tartaric acid with regard to miconazole. The situation is very different with HPβCD and HPγCD in combination with L-tartaric acid because the formation of the ternary complex will be preferential maybe because the large size of the molecular system allows the simultaneous interaction between, on one hand, miconazole and HPCD and between, the acid and the HPCD on the other hand.

4. Conclusion

This study clearly demonstrates the interactions between acids and βCD. ^{1}H NMR spectroscopy gives an unambiguous proof of the formation of inclusion complexes for the three tested acids. The molecular modeling study at the AM1 level shows that all the complexes are thermodynamically stable and allows the calculation of infrared spectra for the complexes. Some modifications between the infrared spectra of the physical mixtures and the complexes produced by supercritical carbon dioxide processing suggest the formation of genuine inclusion complexes. The comparison between the calculated and the experimental spectra of the acid/βCD complexes confirms this hypothesis.

At the end of this study, the complete role of the acid on the miconazole inclusion is evidenced. Indeed, in function of both the CD and the acid types, the acid can either promote the miconazole inclusion by formation of ternary complex or play a competitive role hindering the formation of miconazole complex or destabilizing the miconazole complex.

Acknowledgment

This work was supported in part by the Belgian program on Interuniveristy Poles of Attraction initiated by the Belgian State, Prime Minister's Office, Services fédéraux des affaires scientifiques, techniques et culturelles (PAI no. P4/03), the Fonds de la Recherche Scientifique Médicale Belge (FRSM, contrat no. 3.4531.92). Geraldine Piel is a scientific research worker supported by the Fonds National de la Recherche Scientifique (Brussels, Belgium). Georges Dive is a research associate of the Fonds National de la Recherche Scientifique. Michel Frederich is a research associate of the Fonds National de la Recherche Scientifique.

References

Barillaro, V., Bertholet, P., Henry de Hassonville, S., Ziémons, E., Evrard, B., Delattre, L., Piel, G., 2004. Effect of acidic ternary compounds on the formation of miconazole/cyclodextrin inclusion complexes by means of supercritical carbon dioxide. J. Pharm. Pharm. Sci. 7, 378–388.

Barillaro, V., Dive, G., Bertholet, P., Evrard, B., Delattre, L., Eric, Z., Piel, G., 2007. Theoretical and experimental investigations on miconazole/cyclodextrin/acid complexes: molecular modeling studies. Int. J. Pharmaceut. 342, 152–160.

Bertholet, P., Gueders, M., Dive, G., Albert, A., Barillaro, V., Perly, B., Cataldo, D., Piel, G., Delattre, L., Evrard, B., 2005. The effect of cyclodextrins on the aqueous solubility of a new MMP inhibitor: phase solubility, ^{1}H NMR spectroscopy and molecular modeling studies, preparation and stability study of nebulizable solutions. J. Pharm. Pharm. Sci. 8, 164–175.

Bononi, L.J. 1990. β-cyclodextrin complexes of miconazole and econazole. Bononi & C.Gruppo di Ricerca Srl. 579084[US5422347] Italy, 5-9-1990.

Csernàk, O., Buvàri-Barcza, A., Samu, J., Barcza, L., 2005. Uncommon interactions of aliphatic dicarboxylic acids with cyclodextrins. J. Incl. Phenom. Macro. 51, 59–63.

Dewar, M.J.S., Zoebisch, E.G., Healy, E.F., Stewart, J.P.P., 1985. AM1: a new general purpose quantum mechanical molecular model. J. Am. Chem. Soc. 107, 3902–3909.

Dive, G., Dehareng, D., Ghuysen, J.M., 1993. Energy analysis on small to medium sized H-bonded complexes. Theor. Chim. Acta 1993, 409–421.

Djedaïni, F., Perly, B., 1990. Nuclear magnetic resonance of cyclodextrins, derivatives and inclusion compounds. In: Duchêne, D. (Ed.), New Trends in Cyclodextrins and Derivatives. Editions de Santé, Paris.

Fenyvesi, E., Vikmon, M., Szeman, J., Redenti, E., Delcanale, M., Ventura, P., Szejtli, J., 1999. Interaction of hydroxy acids with β-cyclodextrin. J. Incl. Phenom. Macro. 33, 339–344.

Frisch, M.J., Trucks, G.W., Schlegel, H.B., Scuseria, G.E., Robb, M.A., Cheeseman, J.R., Zakrzewski, V.G., Montgomery, J.A., Stratmann, R.E., Burant, J.C., Dapprich, S., Millam, J.M., Daniels, A.D., Kudin, K.N., Strain, M.C., Chen, W., Farkas, O., Tomasi, J., Barone, V., Cossi, M., Cammi, R., Mennucci, B., Pomelli, C., Adamo, C., Clifford, S., Ochterski, J., Petersson, G.A., Ayala, P.Y., Cui, Q., Morokuma, K., Malick, D.K., Rabuck, A.D., Raghavachari, K., Foresman, J.B., Ciolowski, J., Oritz, J.V., Baboul, A.G.G.,

Stefanov, B.B., Liu, G., Liashenko, A., Piskorz, P., Komaromi, I., Gomperts, R., Martin, R.L., Fox, D.J., Keith, T., Al-Laham, M.A., Peng, C.Y., Nanyakkara, A., Gonzalez, C., Challacombe, M., Gill, P.M.W., Jonhson, B., Wong, M.W., Andres, J.L., Head-Gordon, M., Replogle, E.S., Pople, J.A. 1998. Gaussian 98, A 7.

Germain, P., Bilal, M., de Brauer, C., 1995. β-cyclodextrin/citric acid complexation equilibrium: thermodynamic study. Apparent solubility of βCD in aqueous solutions of citric acid. Thermochim. Acta 259, 187–198.

Gorelsky, S.I., 2005. SWizard Pprogram [4.1]. Stanford University, Stanford.

Henry de Hassonville, H., Dive, G., Evrard, B., Barillaro, V., Bertholet, P., Delattre, L., Piel, G., 2004. Application of molecular modeling to the study of cyproterone acetate stability in the presence of cyclodextrin derivatives. J. Drug Deliv. Sci. Technol. 14, 357–362.

Holder, A.J., Barley, C.W., 1993. An AM1 semiempirical molecular orbital investigation of the group 14 [1.1.1] propellanes and bicyclo[1.1.1]pentanes. Theochem-J. Mol. Struct. 281, 131–139.

Loftsson, T., Brewster, M.E., 1996. Pharmaceutical applications of cyclodextrins, 1. Drug solubilization and stabilization. J. Pharm. Sci. 85, 1017–1025.

Mc Quarrie, D.A., 1973. Statistical Thermodynamics. Harper & Row, New-York.

Mura, P., Liguori, A., Bramanti, G., Bettinetti, G.P., Campisi, E., Faggi, E., 1992. Improvement of dissolution properties and microbiological activity of miconazole and econazole by cyclodextrin complexation. Eur. J. Pharm. Biopharm. 38, 119–123.

Piel, G., Dive, G., Evrard, B., Van Hees, T., Henry de Hassonville, S., Delattre, L., 2001. Molecular modeling study of β- and γ-cyclodextrin complexes with miconazole. Eur. J. Pharm. Sci. 13, 271–279.

Piel, G., Evrard, B., Fillet, M., Llabres, G., Delattre, L., 1998. Development of a non-surfactant parenteral formulation of miconazole by the use of cyclodextrins. Int. J. Pharm. 169, 15–22.

Redenti, E., Szente, L., Szejtli, J., 2000. Drug/cyclodextrin/hydroxy acid multicomponent systems. Properties and pharmaceutical applications. J. Pharm. Sci. 89, 1–8.

Schaftenaar, G., Noordik, J.H., 2000. Molden: a pre- and post-processing program for molecular and electronic structures. J. Comput. Aid. Mod. Des. 14, 123–134.

Schneider, H.J., Hacket, F., Rudiger, V., Ikeda, H., 1998. NMR studies of cyclodextrins and cyclodextrin complexes. Chem. Rev. 98, 1755–1786.

Scott, A.P., Radom, L., 1996. Harmonic vibrational frequencies: an evaluation of Hartree–Fock, Moller–Plesset, quadratic configuration interaction, denity functionnal theory, and semiempirical scale factors. J. Phys. Chem. A 100, 16502–16513.

Suzuki, M., Ito, K., Fushimi, C., Kondo, T., 1993. A study of cyclodextrin complex formation by a freezing point depression method. Chem. Pharm. Bull. 41, 942–945.